



## **UWL REPOSITORY**

**repository.uwl.ac.uk**

Shear behavior of reinforced concrete continuous deep beams

Shaaban, Ibrahim ORCID logo ORCID: <https://orcid.org/0000-0003-4051-341X> (2012) Shear behavior of reinforced concrete continuous deep beams. In: Proceedings of 8th Asia Pacific Structural Engineering and Construction Conference (APSEC 2012), 2-4 Oct 2012, Indonesia.

**This is the Accepted Version of the final output.**

**UWL repository link:** <https://repository.uwl.ac.uk/id/eprint/6971/>

**Alternative formats:** If you require this document in an alternative format, please contact: [open.research@uwl.ac.uk](mailto:open.research@uwl.ac.uk)

### **Copyright:**

Copyright and moral rights for the publications made accessible in the public portal are retained by the authors and/or other copyright owners and it is a condition of accessing publications that users recognise and abide by the legal requirements associated with these rights.

**Take down policy:** If you believe that this document breaches copyright, please contact us at [open.research@uwl.ac.uk](mailto:open.research@uwl.ac.uk) providing details, and we will remove access to the work immediately and investigate your claim.

### **Rights Retention Statement:**

# Shear Behavior of Reinforced Concrete Continuous Deep Beams

Associate Professor: Fouad B. A. Beshara  
Civil Engineering Department  
Shoubra Faculty of Engineering,  
Benha University  
Cairo, Egypt  
foush59@yahoo.com

Professor: Ibrahim G. Shabaan  
Civil Engineering Department  
Shoubra Faculty of Engineering,  
Benha University  
Cairo, Egypt  
igshaaban@mailier.scu.eun.eg

Assistant Lecturer: Tarek S. Mustafa  
Civil Engineering Department  
Shoubra Faculty of Engineering,  
Benha University  
Cairo, Egypt  
eng\_tarek\_sayed@yahoo.com

**Abstract**—Test results of nine reinforced concrete continuous deep beams are presented and analyzed. The main variables studied were shear span-to-depth ratio ( $a/d$ ), vertical web reinforcement ratio ( $\rho_v$ ), horizontal web reinforcement ratio ( $\rho_h$ ), and concrete compressive strength ( $f_{cu}$ ). The results of this study show that the stiffness reduction was prominent in case of lower concrete strength and higher shear span-to depth ratio and that the variation of strains along the main longitudinal top and bottom bars was found to be dependent on the shear span-to depth ratio. For beams having small ( $a/d$ ) ratio, horizontal shear reinforcement was always more effective than vertical shear reinforcement. Finally, the obtained test results are compared to the predictions of finite element analysis using the ANSYS 10 program and a well agreement between the experimental and analytical results was found.

**Keywords**—continuous beams; deep beams; deflection; reinforced concrete; shear strength; web reinforcement

## I. INTRODUCTION

Reinforced concrete (RC) continuous deep beams are fairly commonly used as load distribution elements such as transfer girders, pile caps, tanks, folded plates, and foundation walls, often receiving many small loads and transferring them to a small number of reaction points. There have been extensive experimental investigations of simply supported RC deep beams (Bircher et al. 2011) but very few tests are presented on continuous RC deep beams (Ashour et al. 2008). Continuous deep beams differ from either simply supported deep beams or continuous shallow beams. In continuous deep beams, the regions of high shear and high moment coincide and failure usually occurs in these regions. In simple RC deep beams, the region of high shear coincides with the region of low moment. Failure mechanisms for continuous RC deep beams are therefore significantly different from failure mechanisms in simply supported beams. Deep beams develop a truss or tied arch action more marked than in shallow beams where shear is transferred through a fairly uniform diagonal compression field.

The present paper reports test results of nine two-span RC deep beams (Mustafa 2012). The tested variables were shear span-to-depth ratio, vertical web reinforcement ratio, horizontal web reinforcement ratio, and concrete compressive

strength. The specimens were tested in a compression machine where increasing monotonic static loads were at each mid-span. All tested beams were loaded until failure. The failure planes evolved along the diagonal crack formed at the concrete strut along the edges of the load and intermediate support plates. The test results were measured at different loading levels for the mid-span deflection, mid-span bottom steel strain, middle-support top steel strain, middle-support stirrups strain, and end-support stirrups strain. Also, the cracking patterns were identified. The effects of testing variables on the first diagonal crack load, ultimate shear load, deflection, stiffness, and failure mechanisms were studied. Finally, the obtained test results are compared to the predictions of finite element analysis for continuous deep beams and a well agreement between the experimental and analytical results was found.

## II. EXPERIMENTAL PROGRAM

### A. Test Specimens and Materials

Nine two-span RC deep beams were tested. The overall dimensions of each series are shown in Fig. 1. All tested beams had the same span length and width. The overall length  $L$  was 2000 mm divided by two spans of 1000 mm for each and the width  $b$  was 150 mm. The locations of center lines of loads and supports were the same for all test beams. According to the beam height ( $h$ ) and shear span-to-depth ( $a/d$ ) ratios, the beams were divided into three groups. For tested beams (BS1, BS2, BS3, BS6, and BS9), the height was 500 mm and ( $a/d$ ) ratio was one. For tested beams (BS4, BS5, and BS7) the height was 650 mm and ( $a/d$ ) ratio was 0.77. The height of last beam (BS8) was 400 mm to give ( $a/d$ ) ratio as 1.25. The details of reinforcement and height for each beam are shown in Fig. 2 and table (1). The main longitudinal top and bottom reinforcement was sufficient and kept constant for all tested beams in order to prevent premature flexural failure. All longitudinal bottom steel reinforcement extended the full length of the beams and through the depth to provide sufficient anchorage lengths. The vertical web reinforcement was closed stirrups and the horizontal web reinforcement as longitudinal bars in both sides of the beam. All longitudinal top and bottom reinforcement was 16-mm diameter high-strength steel bars with yield stress of 400 MPa. The web reinforcement was normal mild steel of 8-mm diameter with yield stress of 280

MPa. The amount of vertical and horizontal web reinforcement included three levels. Several trial mixes have been tested to achieve the target compressive concrete strengths of 25 MPa and 35 MPa at 28 days with water/cement ratio (w/c) 0.6 and 0.475, respectively.

### B. Testing Procedure and Instrumentation

Fig. 3 shows the test setup. Special arrangements had been taken to obtain two point loads and three support reactions. A top steel spreader beam was used to divide the total applied load from the machine head into two equal point loads, one in each span. Another stiffer steel beam was placed underneath the tested beams to collect the three support reactions to the other head of the machine. Each beam was tested as a continuous beam under two vertical concentrated loads using a vertical hydraulic jack. The three supports rested on flat plates to combat instability out of the beam plane as shown in Fig. 3. All tested beams were painted by a thin white coat to facilitate the observation and determination of cracks at different stages of loading. With regard to the two vertical loads, they were similar in their acting position, value and were separated by a distance equal 1000 mm. During testing, the vertical loads were applied in increments equal to about 5% of the expected ultimate load and up to failure. After each load increment, marking of cracks was made and the results were recorded automatically using the data logger.

The loads and reactions have been measured using a load cell of capacity 2000kN and 0.1kN accuracy. The load cell readings were recorded automatically using the data logger. The corresponding vertical deflections of test beams at the locations of the mid-span point were measured using LVDT's of 100 mm capacity and 0.01 mm accuracy. Electrical strain gauges of length 10 mm, with resistance  $120.4 \pm 0.4$  ohm, and a gauge factor of 2.11 were used to measure the strains in the main longitudinal top and bottom flexural steel, vertical stirrups, and horizontal shear reinforcement. The gauges were fixed on the steel bars before casting. The surface of the steel was cleaned and smoothed, and the gauges were installed on the steel bars using adhesive material and then they were covered with a water proofing material for protection. For all beams, two gauges were fixed on the top bar at the interior support and on the bottom bar at the mid span. In addition, four gauges were fixed on two vertical stirrups and horizontal shear reinforcement at intersection points of these stirrups and horizontal reinforcement with the strut lines joining the point load with the internal and external supports. The load, deflections, and steel strains were measured and recorded automatically by connecting the load cell, LVDT's, and the electrical strain gauges to data acquisition system.

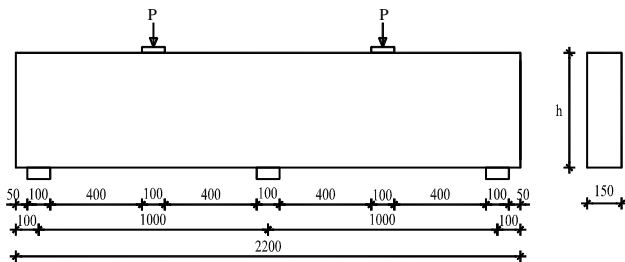


Figure 1. Geometrical dimensions of the tested deep beams (mm)

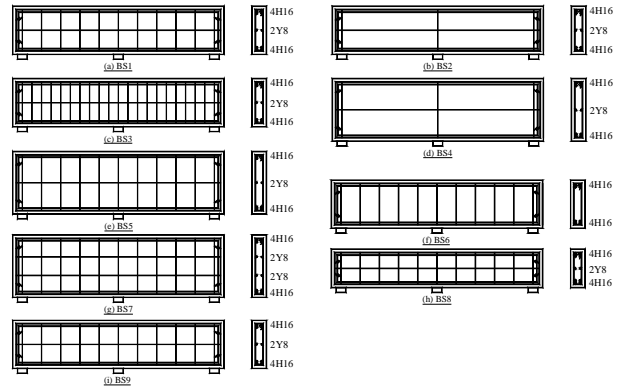


Figure 2. Details of tested RC deep beams

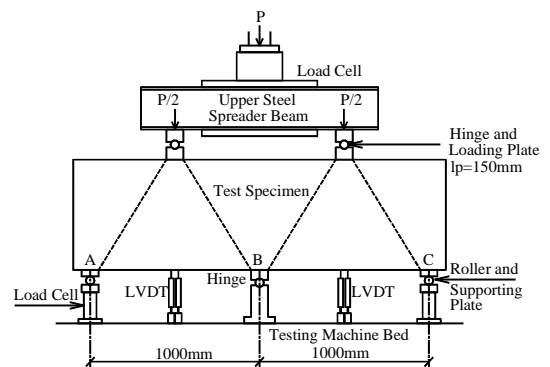


Figure 3. Typical test setup and instrumentation for all tested beams

TABLE I. DETAILS OF REINFORCEMENT FOR THE TEST BEAMS

BEAM	h (mm)	(a/d)	VL RFT	$\rho_v$ (%)	HL RFT	$\rho_h$ (%)	$f_{cu}$ (MPa)
BS1	500	1	Y8@200	0.33	2Y8	0.33	25
BS2	500	1	--	0.0	2Y8	0.33	25
BS3	500	1	Y8@100	0.66	2Y8	0.33	25
BS4	650	0.77	--	0.0	2Y8	0.24	25
BS5	650	0.77	Y8@200	0.33	2Y8	0.24	25
BS6	500	1	Y8@200	0.33	--	0.0	25
BS7	650	0.77	Y8@200	0.33	4Y8	0.48	25
BS8	400	1.25	Y8@200	0.33	2Y8	0.44	25
BS9	500	1	Y8@200	0.33	2Y8	0.33	35

## III. EXPERIMENTAL RESULTS

### A. Specimen Behavior

Fig. 4 shows the cracking patterns at failure for the tested beams (BS1, BS4, and BS8) with (a/d) of 1.0, 0.77, and 1.25 respectively. In the figure, each crack is marked by a line representing the direction of cracking. The crack propagation was significantly influenced by the (a/d) ratio as shown in Fig. 4. Specimens with larger (a/d) showed earlier development of flexural cracks, and a less well defined shear cracks.

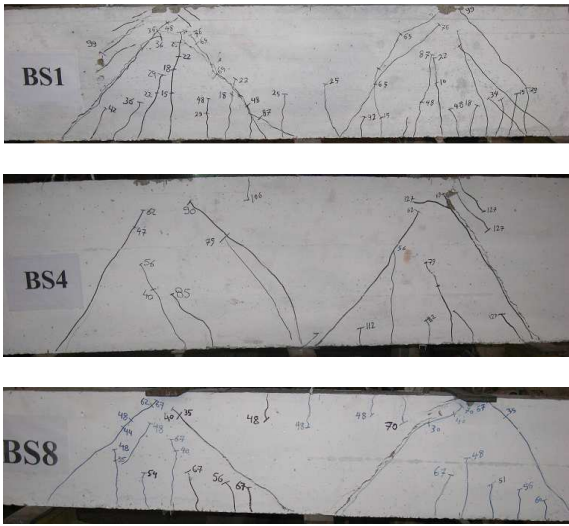


Figure 4. Crack patterns and failure zones of tested beams BS1,BS4,and BS8

Generally, the first crack suddenly developed in the flexural sagging region at approximately 25% of the ultimate strength, and then a crack in the diagonal direction at approximately 30% of the ultimate strength at the mid-depth of the concrete strut within the interior shear span immediately followed. The first flexural crack over the intermediate support generally occurred at approximately 80% of the ultimate strength. As the load increased, more flexural and diagonal cracks were formed and a major diagonal crack extended to join the edges of the load and intermediate support plates. A diagonal crack within the exterior shear span occurred suddenly near the failure load. Just before failure, the two spans showed nearly the same crack patterns. All tested beams developed the same mode of failure as observed in (Ashour et al. 2007). The failure planes were traced along the diagonal crack formed at the concrete strut along the edges of the load and intermediate support plates. Two rigid blocks separated from original beams at failure due to the significant diagonal cracking. The influence of shear reinforcement on the tested beams behavior was not significant as mentioned before in (Singh et al. 2006). In beam without stirrups (BS2), the failure was sudden and was due to crushing of the concrete compression struts. When sufficient stirrups are present, crack fans develop under the loads, and over the interior support; these cracks diminish the effective width of any direct compression strut which might develop.

### B. Mid-Span Deflections

The measured load-deflection curves for all tested beams are shown in Fig. 5. Also, the measured first flexural cracking load at mid-span ( $P_{crfm}$ ), the first flexural cracking load at internal support ( $P_{crfs}$ ), the first diagonal cracking load ( $P_{crs}$ ), and the ultimate total load ( $P_u$ ) are given in Table (2). It can be seen from Fig. 5 and Table (2) that the decrease of (a/d) leads to an increase in the load carrying capacity and stiffness at different levels. The measured deflections indicate that beams with smaller (a/d) ratio exhibit less deformation and ductility than that of higher (a/d) ratio, and as (a/d) ratio decreased; the deflection at the same load level is reduced.

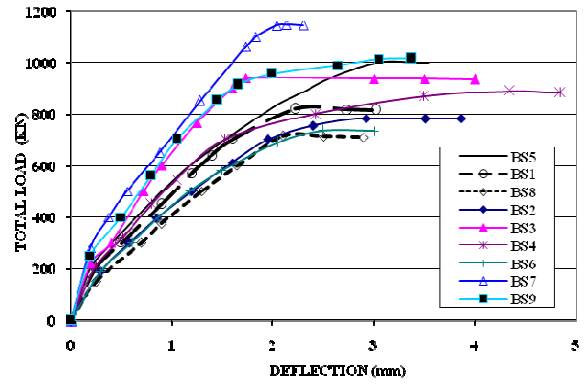


Figure 5. Total applied load and mid-span deflection relationship for the tested beams

TABLE II. EXPERIMENTAL RESULTS OF THE TESTED BEAMS (KN)

BEAM	BS1	BS2	BS3	BS4	BS5	BS6	BS7	BS8	BS9
$P_{crfm}$	200	200	250	300	320	200	370	150	250
$P_{crfs}$	600	585	660	680	740	550	860	540	750
$P_{crs}$	250	240	280	290	340	240	390	220	300
$P_u$	819	782	939	889	1001	735	1145	715	1015
$R_{outer}$	148	141	169	161	181	133	206	129	183
$R_{inner}$	523	500	601	567	639	469	733	457	649
$Q_{uinner}$	262	250	301	284	320	235	367	229	325
$Q_{uACI}$	215	201	255	267	280	175	350	174	245
$Q_{uECP}$	204	191	218	262	277	173	330	169	238

Increasing (a/d) ratio from 1.0 for beam BS1 to 1.25 for beam BS8 resulted in a decrease in  $P_{crfm}$ ,  $P_{crs}$  and  $P_u$  by about 25.0%, 12.0%, and 13.0%, respectively. Furthermore, the enhancement in  $P_{crfm}$ ,  $P_{crs}$  and  $P_u$  is respectively 60.0%, 36.0%, and 22.0% due to decreasing (a/d) ratio from 1.0 for beam BS1 to 0.77 for beam BS3. It can be seen that increasing the concrete compressive strength has a significant improvement effect on the load-deflection response. Increasing the concrete compressive strength led to a more brittle behavior with increased load carrying capacities and stiffness at different load levels. The  $P_{crfm}$ ,  $P_{crs}$  and  $P_u$  were increased respectively by 25.0%, 20.0%, and 24.0% for beam BS9 with ( $f_{cu}$ ) of 35.0 MPa when compared to beam BS1 with ( $f_{cu}$ ) of 25.0 MPa.

The examination of measured results in Fig. 5 and in Table (2) showed that the load carrying capacities at different levels increase with an increase in the ratio of vertical shear reinforcement ( $\rho_v$ ). The tested beam BS2 without stirrups showed a minor reduction in  $P_{crs}$  and  $P_u$  by 4.0% and 5.0% when compared to beam BS1 ( $\rho_v = 0.00335$ ), while the first flexural cracking load was kept the same. On the other hand, the increase in  $P_{crfm}$ ,  $P_{crs}$  and  $P_u$  was found 25%, 12.0%, and 15.0% respectively for beam BS3 having ( $\rho_v$ ) as 0.0067 when compared to beam BS1 with  $\rho_v = 0.00335$ . Fig. 5 also indicates that beam without vertical stirrups had very little ductility and continuous deep beams with heavy stirrups were ductile while those with light stirrups were fairly brittle.

The horizontal shear reinforcement has generally a moderate effect on the improvement of the measured load-deflection response of tested deep beams. From comparison of results in Fig. 5 and Table (2), it was found that there is a

reduction in  $P_{crs}$  and  $P_u$  by 4% and 10% respectively for beam tested BS6 with  $(\rho_h)$  of 0.00 when compared to beam BS1 with  $(\rho_h)$  of 0.0033 with the same  $(a/d)$  while the first flexural cracking load was found the same for both beams. In other comparison, beam BS7 with  $(\rho_h)$  of 0.0048 showed an increase in  $P_{crfm}$ ,  $P_{crs}$  and  $P_u$  by 16.0%, 15.0%, and 14.5% respectively when compared to beam BS5 with  $(\rho_h)$  of 0.0024 while the other parameters were kept constant.

### C. Steel Strains

Figs. 6 and 7 show respectively the load-steel strain curves for bottom and top longitudinal flexural reinforcement of the tested beams. These figures also indicate that tested beams with the same  $(a/d)$  ratio shows almost the same total applied load-strain gradient with major strains redistribution in the bottom steel after the first diagonal cracking. The total applied load-strain gradient shows minor strains redistribution in the top steel after the first diagonal cracking and shows also the same similarity for the beams with the same  $(a/d)$  ratio. The bottom longitudinal reinforcement was in tension throughout the length of the beam, and the top reinforcement was also in tension throughout the length of the interior shear span.

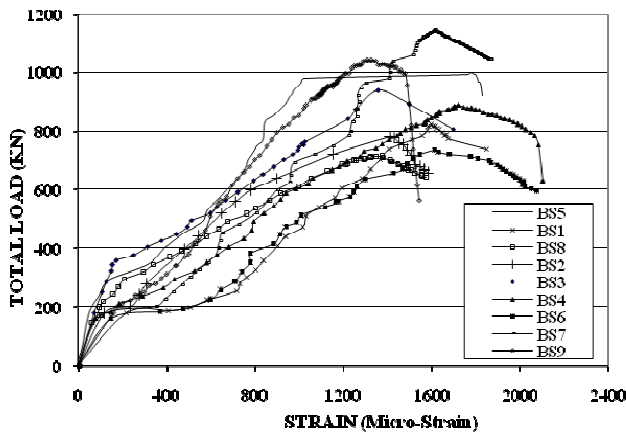


Figure 6. Total applied load and bottom steel strain relationship for the tested beams

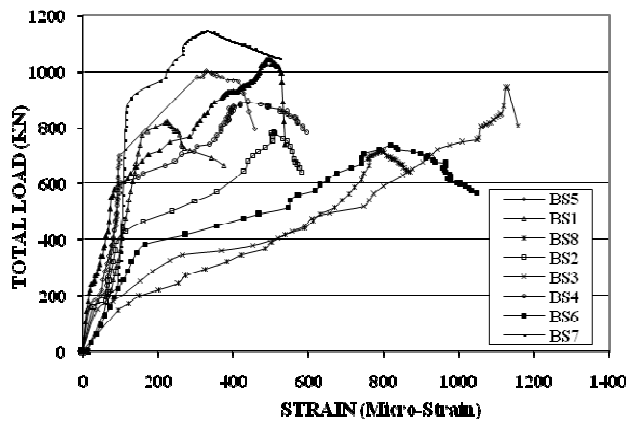


Figure 7. Total applied load and top steel strain relationship for the tested beams

Neither bottom nor top longitudinal flexural reinforcement was yielded up to failure load for the tested beams due to the over reinforced design of flexural reinforcement. Strains in bottom reinforcement were higher than in top steel due to stress redistribution which increases the field moment and decreases the moment at intermediate support. In beam without stirrup (BS2), the flexural reinforcement strains are constant along the bars between point loads and supports and a compression struts develop in the concrete which carry the loads directly to the supports.

The total load-steel strain curves for vertical and horizontal shear reinforcement at the interior shear span for the tested beams are shown in Figs. 8 and 9, respectively. A minor redistribution of strains occurred at the vertical steel after the occurrence of the first diagonal crack for beams BS5 and BS1 having the lower values of  $(a/d)$  ratio as 0.77 and 1.0 respectively and did not yield. A major strain redistribution occurred for beam BS8 having  $(a/d)$  ratio of 1.25 and reached yield at failure. For the horizontal steel, a redistribution of strains occurred after first diagonal cracking for these three beams but this redistribution was higher for beam BS5 having the lowest  $(a/d)$  ratio of 0.77. None of the horizontal reinforcement for the three test beams reached yield up to failure. Comparison of test results indicate that the influence of web steel on the ultimate shear strength is influenced by the  $(a/d)$  ratio, the lower the  $(a/d)$  ratio; the more effective the horizontal steel and the less effective the vertical steel. Only the vertical steel of beam BS3 having a heavy vertical steel ratio reached yield.

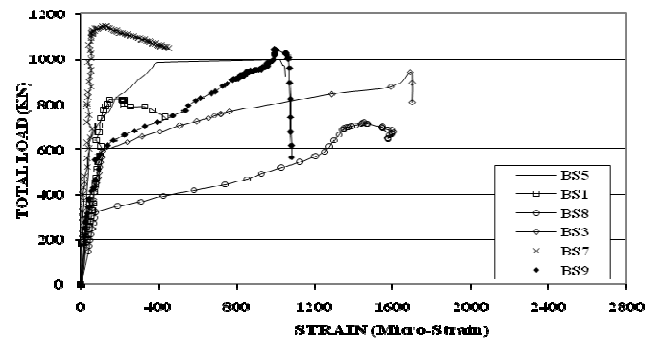


Figure 8. Total applied load and vertical shear reinforcement strain relationship

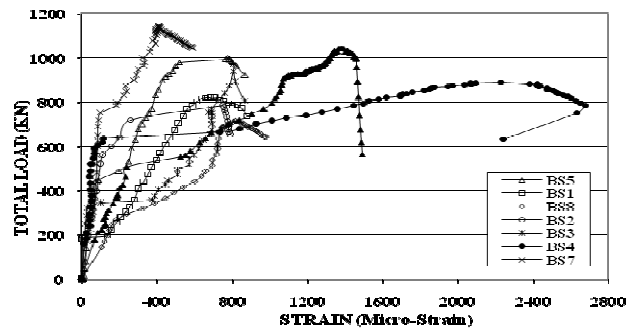


Figure 9. Total applied load and horizontal shear reinforcement strain relationship

It was also concluded that tested beam BS6 without horizontal reinforcement showed a higher values of strains in the vertical reinforcement than beam BS1 with ( $\rho_h$ ) of 0.0033 at the same load level. A major redistribution of strains occurred for the vertical steel at about 70.0% of the ultimate load for beam BS9 but did not yield as the vertical reinforcement for beam BS1. For the horizontal reinforcement, while major strain redistribution was occur for beam BS1 at the first diagonal cracking, similar strain redistribution have been occurred in beam BS9 with higher value of ( $f_{cu}$ ) but at about 50.0% of the ultimate load and this is due to the expected higher value of concrete shear contribution. Horizontal steel for beam BS9 almost reached yield point while beam BS1 did not reach that point.

#### D. Reaction of Supports

The measured amount of load transferred to the end support is listed in Table (2) for all tested beams. From external equilibrium of forces and symmetry, the measured reaction at intermediate support is evaluated in the table. Linear elastic analysis was performed using SAP program for beams in order to assess the reactions of supports. From elastic analysis, the reactions of the exterior and intermediate supports due to the total applied load ( $P$ ) are  $0.175P$  and  $0.65P$  respectively. It was stated before (Ashour et al. 2000) that the differential settlement had no significant effect on the elastic behavior of continuous deep beams, and would have less significance at higher loads in any case. Fig. 10 shows the measured amount of the load transferred to the end and intermediate supports against the total applied load for beams having constant ( $a/d$ ) value of 1.0 and different web reinforcement ratios. On the same figure, the reactions at support are obtained from elastic analysis are also presented. Although the amount of web steel influences the maximum reaction at support, it has no effect on the total load-support reaction gradient. Before the first diagonal crack, the relationship of the end and intermediate support reactions against the total applied load in all tested beams shows good agreement with elastic prediction. The amount of loads transferred to the end support, however, was slightly higher than that predicted by the elastic analysis after the occurrence of the first diagonal crack within the interior shear span. At failure, the difference between the measured end support reaction and prediction of the elastic analysis was in order of 8%, 10%, and 14%, for beams with ( $a/d$ ) of 0.77, 1.0, and 1.25, respectively.

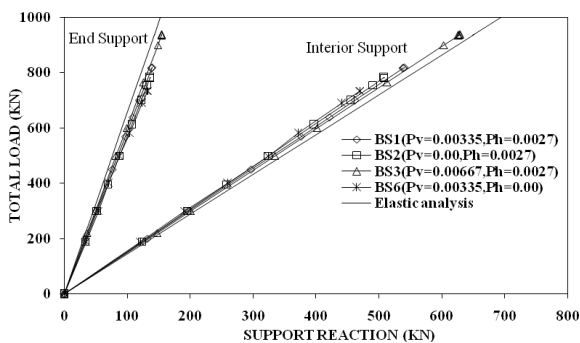


Figure 10. Total applied load versus support reactions for beams having ( $a/d = 1.0$ )

The internal redistribution of forces is limited. Also, the distribution of applied load to supports is independent of the amount and configuration of shear reinforcement. This means that the occurrence of diagonal cracks reduces the beam stiffness and the hogging moment over the central support, and increases the sagging bending moment within the span.

#### E. Experimental Shear Force Capacities and Comparison with Current Codes

The most critical shearing force in continuous deep beams occurs at the interior support. The shear forces at inner supports of tested deep beams ( $Q_{\text{inner}}$ ) are calculated as half the vertical support reactions, and are listed in Table (2). It can be seen that the ultimate shear strength of beams with constant shear reinforcement and concrete strength increase significantly with the decrease of ( $a/d$ ) ratio. The decrease of ( $a/d$ ) ratio from 1.25 (beam BS8) to 1.0 (beam BS1) increases the shear capacity by 14.4%. For beams with vertical shear steel, the drop of ( $a/d$ ) ratio from 1.0 (beam BS1) to 0.77 (beam BS5) enhances the shear capacity by 22.1%. For tested deep beams without vertical shear reinforcement, the drop of ( $a/d$ ) ratio from 1.0 (beam BS2) to 0.77 (beam BS4) enhances the shear capacity by 13.6%. Table (2) indicates that the shear strength for beams with constant ( $a/d$ ) ratio and shear reinforcement increases remarkably with the increase of concrete compressive strength. The shear capacity of beam BS9 with  $f_{cu} = 35$  MPa is higher than that of beam BS1 with  $f_{cu} = 25$  MPa by 24%. The analysis of experimental results indicates that the ultimate shear strength increases with the increase of amount of vertical or horizontal shear reinforcement for different ( $a/d$ ) ratios. For beams with ( $a/d$ ) = 1.0, the increase of  $\rho_v$  from zero (beam BS2) to 0.0033 (beam BS1) and to 0.0066 (beam BS3) enhances the shear capacity by 5% and 20.4%, respectively. For beams (BS4 & BS5) with ( $a/d$ ) = 0.77, the increase in  $\rho_v$  by 0.0033 increases the shear capacity by 12.7%. Previous test results of simple deep beams (Brown et al. 2007) have suggested that horizontal shear reinforcement has little effect on the shear strength improvement. In current test results, horizontal shear steel has a moderate effect on shear carrying capacity, especially for beams with ( $a/d$ ) < 1. For beams (BS5 & BS7) with ( $a/d$ ) = 0.77, the shear strength improvement was 14.7% due to 0.0024 increase in  $\rho_h$  ratio. For beams (BS1 & BS6) with ( $a/d$ ) = 1, the same increase in  $\rho_h$  ratio improves the shear capacity by 12.7%.

The prediction of shear capacity of tested beams was shown in Table (2) using two design codes; namely (ACI 318-08) and the Egyptian concrete code of practice (ECP-203-2007). The shear contributions from concrete, horizontal, and vertical shear reinforcement were evaluated with all safety factors removed. Both design methods show that the amount of shear resisted by horizontal steel is higher than that resisted by vertical steel (contrary to testing results). This prediction indicates that ACI as well as ECP underestimate the shear capacity for continuous deep beams. The average ratios of ( $Q_{\text{inner}} / Q_{u\text{ACI}}$ ) and ( $Q_{\text{inner}} / Q_{u\text{ECP}}$ ) are 1.21 and 1.27 with standard deviations of values 0.11 and 0.12, respectively. The discrepancy in codes predictions may be attributed to the fact that the shear strength equations in both design methods for continuous deep beams are derived from simple deep beam tests.

#### IV. FINITE ELEMENT PREDECTIONS

The nonlinear finite element program; ANSYS 10 was used to predict the behavior of tested deep beams. A correlative study based on the load- deflection response as well as the cracking patterns was conducted to verify the analytical model with the obtained experimental results. In the finite element discretization of the tested beams, a 50x50 mm mesh of eight-node brick elements (Element 65) was used for concrete. The top & bottom flexural steel bars and the horizontal & vertical web reinforcement were represented by bar elements. The area and spacing of such bar elements were similar to the experimental specimens. The concentrated loads were also applied to the top surface at mid-span of the tested beams. The supports were represented by restrained nodes at the corresponding locations. To model concrete behavior, nonlinear stress-strain curves were used in compression and tension. Such models account for compression & tension softening, tension stiffening and shear transfer mechanisms in cracked concrete. An elasto-plastic model was used for steel in compression and tension. The initial Young's modulus in concrete was taken as 22 GPa and the steel modulus was 200 GPa. An incremental-iterative technique was employed to solve the nonlinear equilibrium equations. The load increment was set at 5% of the experimental ultimate load. The load increment was subject to adjustment to obtain results at certain specific load levels. The maximum number of iterations was set to 20 in each load step and the equilibrium tolerance of 0.5% was chosen.

The computed cracking patterns at different loading levels are presented for tested beams BS5 and BS8 respectively. Both specimens had the minimum amount of stirrups with (a/d) ratio as 0.77 and 1.25 respectively. Fig. 11 shows the development of the crack pattern in tested beam BS5. First flexural cracking at mid-span (load level 250 kN) was predicted first by the simulation. Beyond this flexural crack, a shear crack band developed (load level 290 kN). After the formation of the crack band, a rather stable crack pattern is formed. The width of shear crack band increased with an increase of the load (load levels: 400-800 kN) in a stable manner.

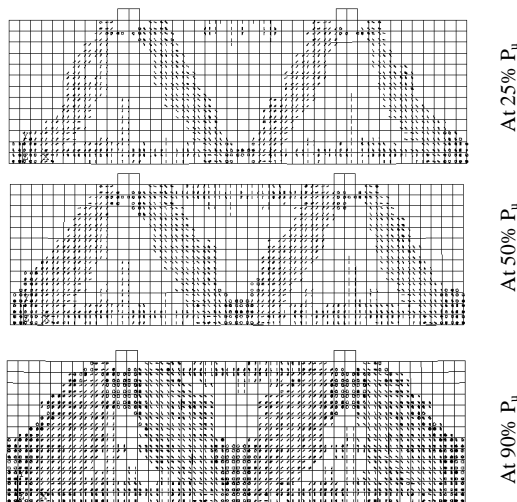


Figure 11. Simulated crack propagation for tested beam BS5

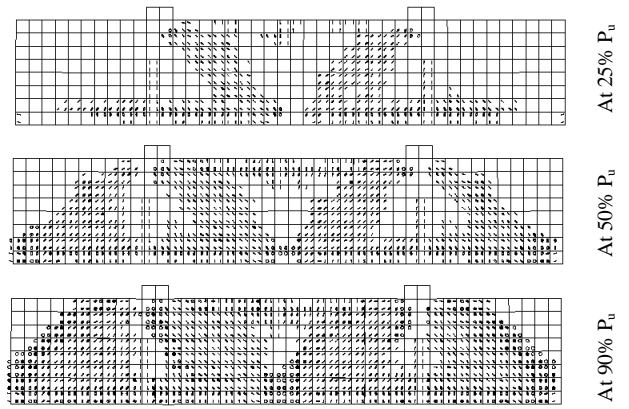


Figure 12. Simulated crack propagation for tested beam BS8

Later, flexural cracking takes place over the middle support. At ultimate stage, failure is initiated by crushing of the concrete in the region adjacent to the middle support (load level 910 kN). There is a good agreement between the simulated crack patterns and the obtained experimental ones. The simulation also successfully predicted the sequence in the crack patterns development and the failure mechanism.

As shown in Fig. 12, the development of the crack pattern for tested beam BS8 with (a/d) ratio of 1.25 is nearly the same as that for tested beam BS5 with (a/d) ratio of 0.77. Compared to BS5, the load levels at which cracks takes place are lower due to increasing (a/d) ratio. First flexural cracking was firstly developed at the mid-span (load level 130 kN) and later over the middle support. At a load level of 170 kN, inclined flexural cracks develop. Afterwards, shear cracking takes place. With further load increase, some secondary flexural cracks are detected. At ultimate stage, the deep beams failed by crushing of the concrete in the regions adjacent to the middle support and the loading point. The simulated and the experimental crack patterns are compared at ultimate load level and it is clear that the finite element analysis simulates the experimental results very well. This can be seen in the internal shear span; going from the middle support to the loading point, the crack direction changes from vertical to inclined, stays constant, and changes back to vertical again.

In Fig. 13, test results of total load- deflection curves are compared to the predictions of finite element analysis for tested beams BS1, BS2 and BS8. A good agreement between the experimental and analytical results was obtained at different levels. In simulated curves, there is a sudden increase in the deflection and this is back to formation of the first flexural crack. Also, formation of the first diagonal crack significantly reduced the beam stiffness. Similar to experimental results, simulated curves are significantly affected by the shear span-to-depth ratio. It can be seen from Fig. 13 that the decrease of (a/d) leads to an increase in the load carrying capacity at different levels. All analyzed beams exhibited limited displacement ductility at failure. The degree of ductility varied depending on the (a/d) ratio where the lower (a/d) ratio, the lower is amount of ductility.

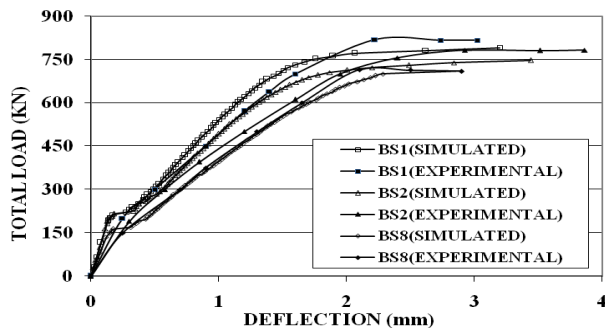


Figure 13. Simulated and experimental load-deflection curves for BS1, BS2, and BS8

Increasing either vertical or horizontal shear reinforcement led to an increase in the analytical load carrying capacity and ductility matching with the experimental results. Increasing the concrete compressive strength has a significant improvement effect on the load-deflection response and there is an increase in the first flexural cracking, first diagonal cracking, and ultimate loads.

### CONCLUSIONS

From the experimental and the analytical studies in the present work, the following conclusions are drawn:

- Deep RC beams with smaller ( $a/d$ ) ratio exhibit higher load carrying capacity, less deformation, and lower ductility than that of higher ( $a/d$ ) ratio. Increasing concrete compressive strength leads to a more brittle behavior with increased load carrying capacity and stiffness at different levels. Deep RC beams with different variables developed the same mode of failure. The failure planes were traced along the diagonal crack formed along the edges of load and intermediate support plates.
- Tensile strains in bottom flexural reinforcement were higher than in top flexural steel due to internal stress redistribution. The lower the ( $a/d$ ) ratio, the less variation is observed. For the vertical web reinforcement, a major redistribution of strains occurred for tested deep beams with ( $a/d$ )  $> 1$  only. For the horizontal web reinforcement, major strain redistribution occurred for beams with ( $a/d$ )  $< 1$ .
- The ultimate shear strength of continuous beams increases significantly with the decrease of the ( $a/d$ ) ratio, and the increase of concrete compressive strength or vertical web reinforcement. The shear capacity of horizontal web steel was more prominent in continuous beams than that in simple ones, especially for beams with ( $a/d$ )  $< 1$ . Due to the limited internal redistribution of forces, the support reaction at interior support is slightly lower than that predicted by linear analysis.

- The comparison between the obtained experimental results and the predictions of the ACI-318-08 and ECP-203-2007 codes indicated that current design codes underestimate the shear capacity of continuous deep beams. This may be attributed to the fact that the shear strength equation in both codes was derived from simple deep beams tests. Contrary to testing results, current design methods predict that shear resistance of horizontal web steel is higher than that of vertical steel.
- The predictions of load-deflection response as well as the cracking patterns using the nonlinear finite element program, ANSYS 10, show a good agreement with the testing results. The finite element predicted successfully the ultimate loads, displacement ductility, stiffness changes and failure mechanisms for deep RC beams with different variables.

## REFERENCES

- ACI Committee 318 (2008) Building code requirements for structural concrete (ACI 318-08) and Commentary (ACI 318-R-08), ACI. *Structural Engineering*.
- Ashour, A.F. and Rishi, G. (2000) Tests of reinforced concrete continuous deep beams with web openings, *ACI Journal. Structural Engineering*, 97: 418-426.
- Ashour, A.F. and Yang, K.H. (2007) Influence of shear reinforcement on reinforced concrete continuous deep beams, *ACI Journal. Structural Engineering*, 104: 420-429.
- Ashour, A.F. and Yang, K.H. (2007) Influence of inclined web reinforcement on reinforced concrete deep beams with openings, *ACI Journal. Structural Engineering*, 104: 580-589.
- Ashour, A.F. and Yang, K.H. (2008) Effectiveness of web reinforcement around openings in continuous concrete deep beams, *ACI Journal. Structural Engineering*, 105: 414-424.
- Brown, M.D. and Bayark, O. (2007) investigation of deep beams with various load configurations, *ACI Journal. Structural Engineering*, 104: 611-620.
- Egyptian Code of Practice (2010) Design and Construction of Reinforced Concrete, Ministry of building construction. *Structural Engineering*.
- Hong, S.H. and Hong, N.K. (2011) deformation capacity of structural concrete in disturbed regions, *ACI Journal. Structural Engineering*, 108: 267-276.
- Matsuo, M. and Yanagawa, A. (2002) shear behavior of RC deep beams with stirrups, *Transactions of the Japan Concrete Institute. Structural Engineering*, 23: 385-390.
- Mihaylov, B. and Collins, M. (2010) Behavior of large deep beams subjected to monotonic and reversed cyclic shear, *ACI Journal. Structural Engineering*, 107: 726-734.
- Mustafa, T.S. (2012) *Behavior of Reinforced Concrete Continuous Deep Beams*. Ph.D. Thesis to be submitted, Faculty of Engineering at Shoubra, Benha University, Egypt.
- Nathan, C.R. and Sergio, F.B. (2008) Behavior of deep beams with short longitudinal bar anchorages, *ACI Journal. Structural Engineering*, 105: 460-470.
- Singh, S.K. and Kaushik, K.F. (2006) Design of a continuous deep beam using the strut-and-tie method, *Asian Journal. Civil Engineering*, 7: 461-477.
- Tuchscherer, R. and Bayark, O. (2011) Distribution of Stirrups across Web of Deep Beams, *ACI Journal. Structural Engineering*, 108: 108-115.
- Walraven, A. (2000) *The Behavior of Reinforced Concrete Continuous Deep Beams*. Ph.D. Thesis, Delft University Press, Netherlands, 156 pp.
- Yang, K.H. (2010) Tests on lightweight concrete deep beams, *ACI journal. Structural Engineering*, 107: 663-670.
- Yang, K.H. Eun, H.C. (2006) The influence of web openings on the structural behavior of reinforced high-strength concrete deep beams, *Engineering Structures. Structural Engineering*, 28: 1825-1834.
- Yang, K.H. Eun, H.C. (2003) Shear characteristics of high-strength concrete deep beams without shear reinforcements, *Engineering Structures. Structural Engineering*, 25: 1343-1352.
- Yang, K.H. (2002) *Evaluation on the Shear Strength of High-Strength Concrete Deep Beams*. Ph.D. Thesis, Chungang University, Korea, 120 pp.